Influence of Barrel Wear and Thermal Deformation on Projectile Ramming Process

JIRI BALLA, STANISLAV PROCHAZKA and VAN YEN DUONG
Department of Weapons and Ammunition
University of Defence
Kounicova 65, 662 10 Brno
CZECH REPUBLIC
jiri.balla@unob.cz, stanislav.prochazka@unob.cz, yen.duongvan@gmail.com

Abstract: - This article deals with barrel wear and barrel thermal deformation of heavy guns and their influence on the ramming process. Barrel wear was measured on 125 mm smooth tank cannon barrels. Barrel thermal deformation and the ramming process of APFSDS projectiles was calculated using ANSYS Workbench software utilising the Finite Element Method (FEM). The ramming process calculation was done for two case scenarios: the first case was for a new barrel deformed by barrel thermal effects from firing; the second case was for a worn barrel influenced by the same thermal effects. The calculation and simulation results were used as a theoretical background for: evaluation of the influence of both barrel thermal deformation and barrel wear on ramming process characteristics; evaluation of firing safety of guns having worn barrels according to the Czech Defence Standards; evaluation and specification of barrel quality of self-propelled howitzers and tank cannons with respect to the ramming process.

Key-Words: - Artillery loading, ramming process, barrel temperature, barrel thermal deformation

1 Introduction

It is known that the combat efficiency of artillery, especially self-propelled howitzers and tanks depends on many tactical and technical factors. One of the most important technical factors is the rapidity of fire and the safety of projectile ramming during unstable motion of fighting vehicles on the battlefield. A very important factor is the safety of projectile ramming while a fighting vehicle in the battlefield is moving fast and over bad terrain or bad road conditions when a heavy projectile must not fall down from the cartridge chamber, see [1], [2], and [3]. Therefore, both the rapidity and safety of ramming depend on the quality of the loading device which is a very important part of the ramming device. Firstly, the ramming device secures the projectile in the barrel while the projectile is engraved into the barrel forcing cone, thus preventing the risk of projectile fall-back. Secondly, the ramming process creates a deformation field between the driving band and the forcing cone to seal the air-gap between the powder chamber and the guidance section of the barrel, ensuring the powder gas does not leak through this air-gap when firing. Thirdly, the accurate position of the projectile in the chamber after ramming gives a steady movement to the projectile in the barrel and decreases vibration of the projectile which, together with all the above mentioned factors, increases firing accuracy. The position of the APFSDS (Armour-Piercing Fin-Stabilised Discarding Sabot) projectile position is illustrated in Fig. 1, see [1], and [4].

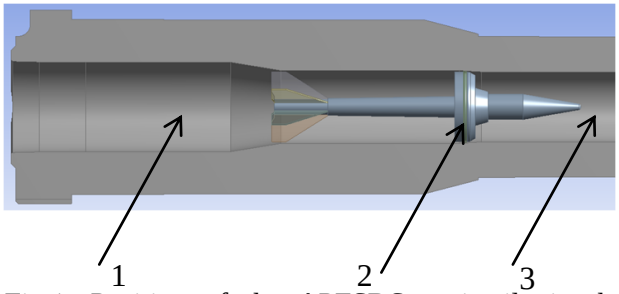

Fig.1: Position of the APFSDS projectile in the barrel after ramming: 1- chamber; 2- contact area between the forcing cone and the driving band; 3- guidance section

The main ramming characteristics are the ramming velocity at the end of the ramming process, when the projectile engraves into the forcing cone, and the ramming force that secures the projectile in the barrel before firing. The ramming velocity has been discussed in [5], [6], [7], and [8], but the determination of ramming forces is very difficult

ISBN: 978-1-61804-141-8

due to the nonlinear plastic-elastic problem making the determination of many factors difficult. The Standard [9] deals with the determination of the force necessary to hold the projectile in the barrel. However, it only defines the opposite force (which must be the same) when the tested projectile is extracted from the barrel using a special arrangement. The first calculated results have been published in [7]. The rammer velocities at the end of the operation obtained from measuring are about 2.9 m/s for the 125 mm tank cannon. The extracting force varies from 15 to 17 kN for the same weapon and the same APFSDS projectile [6].
Barrel wear and thermal deformation influence the ramming process intensively [8] [10], [11], [12], and [13]. In the following section a ramming process with respect to barrel bore wear and the thermal deformation caused by the effects of a firing cycle will be calculated using ANSYS software.

2 Barrel Thermal Deformation

One of the most important side-effects of a shot is barrel heating. Very often it becomes a barrier to the power growth of the weapon. The heat is transferred from the inner surface to the outer surface of the barrel wall. The created uneven thermal field causes on one hand a thermal deformation field and on the other hand thermal expansions due to the temperature rise. The resultant deformation that results from the stress is significantly smaller than the bore expansion, as the thermal expansion is only 10% of the total deformation once the required stabilized temperature state is reached [13]. The radial deformation changes in the barrel along the barrel axis are very important input data for the ramming problem, especially the diameter change of the forcing cone and of the beginning of the leading part (the first third of the forcing cone). The changes in the inner diameter influence the interaction process between the projectile driving band and the forcing cone during ramming.
In order to calculate the thermal deformation field in the barrel wall the Steady-State Thermal component of the ANSYS Workbench software has been used. It is assumed that temperature distribution in the barrel wall is dependant on the radius according to the Fourier-Kirchhoff partial differential equation, describing thermal transmission in the radius direction at a steady temperature mode.

$$T(r) = T_1 - \Delta T \frac{\ln \frac{r}{r_1}}{\ln \frac{r_2}{r_1}}, \qquad (1)$$

Where
T_1 –temperature at the barrel bore,
ΔT – temperature gradient in the barrel wall in the radius direction,
r_1, r_2 – barrel internal and external radius.

The results of the calculations are the heat fields in the barrel wall. These heat fields are used as input data for using the Static Structural component of the ANSYS Workbench software to calculate the thermal deformation fields.

The FEM model for the tank cannon barrel was worked out using [3], and [14] and is shown in Fig. 2. The circle indicated as *a* represents the forcing cone area.

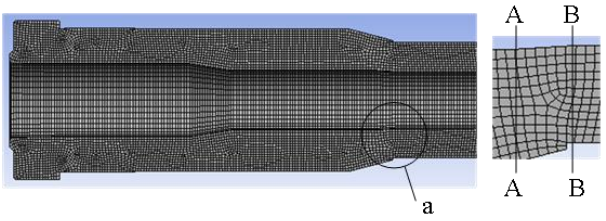

Fig.2: FEM model of a 125 mm tank cannon barrel

The results of calculations have been tested by way of comparison with the analytical solution of the heavy-walled barrel. The boundary conditions at the end of the calculated area were set from the conditions of non-deformation area in the axial direction outside of the calculated area.
The interactions between the projectile driving band and the forcing cone occur in the A-A and B-B cross-sections.
Temperature distribution from the inner surface to the outer surface is shown in Fig. 3. The temperature on the inner surface is, from experience, set at 350°C taking into account the requirement not to exceed the maximum recommended temperature on this surface. The temperature decreases in the radial direction from the inner to the outer surface. The temperature gradient, at the steady temperature state, reaches 150° – 200°C for heavy gun barrels, see [13], and [15]. In this case the temperature on the outer surface was calculated as 200°C. The calculated temperature fields - see Fig. 3 - create the input data for the barrel deformation problem.
The calculation results of barrel thermal deformation are shown in Fig. 4.

ISBN: 978-1-61804-141-8

After each shot, the shape of the barrel forcing cone is changed due to the barrel's thermal deformation. This change forms a new shape in the barrel forcing cone. The calculation results of the radial thermal deformation in A-A and B-B cross section are approximately 0.3 mm (see Fig. 2).

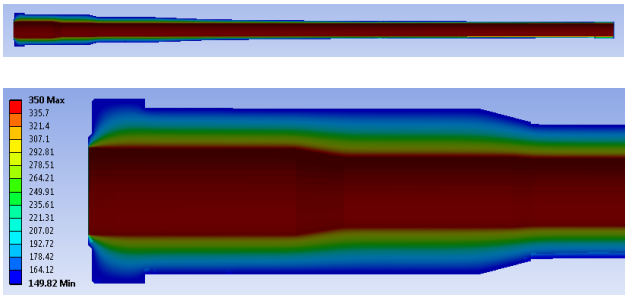

Fig. 3: Temperature field in barrel wall

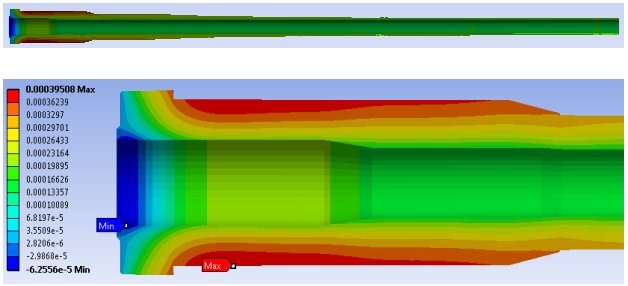

Fig.4: Radial thermal deformation field (m) of barrel wall

The radial thermal deformation of the barrel inner surface along the barrel axis is shown in Fig. 5, where the maximum values are around the forcing cone of the barrel. Those are the danger areas for securing the projectile in the barrel post-ramming, see [10], [11], and [15].

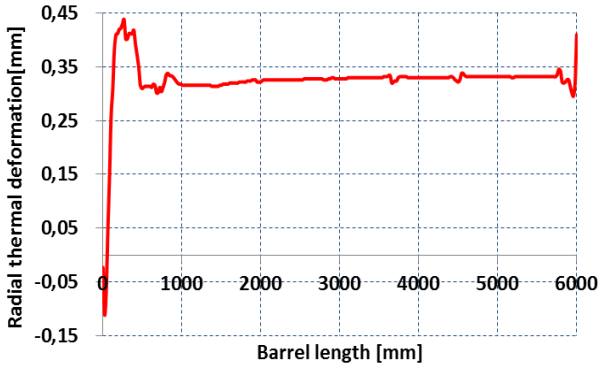

Fig.5: Barrel radial thermal deformation of the inner surface along the barrel length

3 Barrel Wear

The ramming process is influenced not only by barrel thermal deformation, but also by barrel wear that influences projectile ramming more intensively than barrel thermal deformations. This can be explained by the main reason that rapidity of fire of self-propelled howitzers as well as tank cannons is quite low (6 to 8 rounds/min). The time from previous firing cycle to the next firing cycle is quite long with respect to the duration of barrel temperature drop. The barrel temperature drops and the elastic thermal deformations of the barrel disappear or reduce to zero before the next firing cycle is performed. However, in order to satisfy the safety requirements of any weapon system operation, the ramming process with simultaneous influences of barrel thermal deformations and barrel wear will be researched.

Measurement results for the 125 mm worn cannon barrels performed by the Department of Weapons and Ammunition are shown in Fig. 6 and Fig. 7. The inner diameter of the new cannon barrel bore is $125^{+0.15}$ mm.

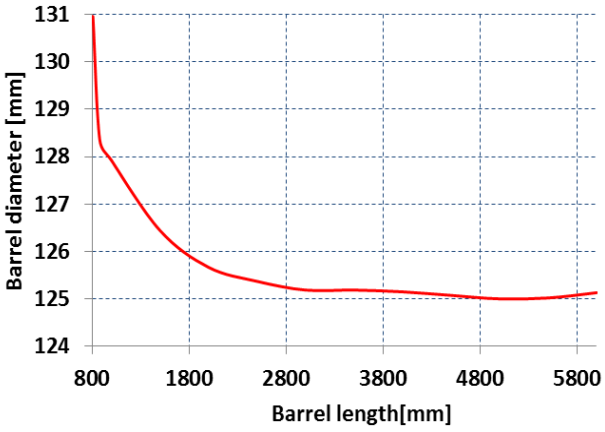

Fig.6: Wear of cannon barrel bore firing mainly APFSDS projectiles with nonferrous sabot

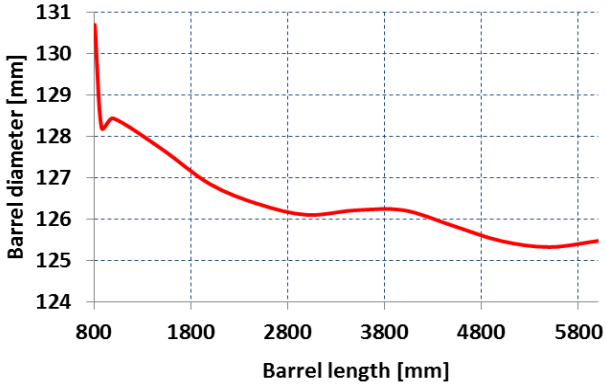

Fig.7: Wear of cannon barrel bore firing HE and APFSDS projectiles with ferrous sabot

The growth of the wear behind the forcing cone in the Fig.7 has been discussed in [5], [6], and [15].

The differences of driving band shape between APFSDS and HE (high explosive) projectiles, quantity of fired rounds etc. cause the barrels wear

ISBN: 978-1-61804-141-8

to be in the different range of values. The barrel that fires HE and APFSDS projectiles is worn out more intensively than the barrel firing new APFSDS projectiles using the nonferrous sabots.
Evidently, barrel wear occurs more intensively at the region of the forcing cone and at the beginning of the elongating part of the barrel bore (the first third of the forcing cone). Therefore, this wear influences the engraving of the projectile at the end of the ramming process, see the next section.

4 Influences of Barrel Thermal Deformation and Barrel wear on Projectile Engraving

The Transient Structural component of the ANSYS Workbench software will simulate the ramming process and calculate its dynamic characteristics.
The calculation and simulation have been carried out for two cases.
The position of the projectile in the barrel with the driving band is marked by the red circle in Fig. 8. The FEM model of the ramming problem is shown in Fig. 9 after magnification.

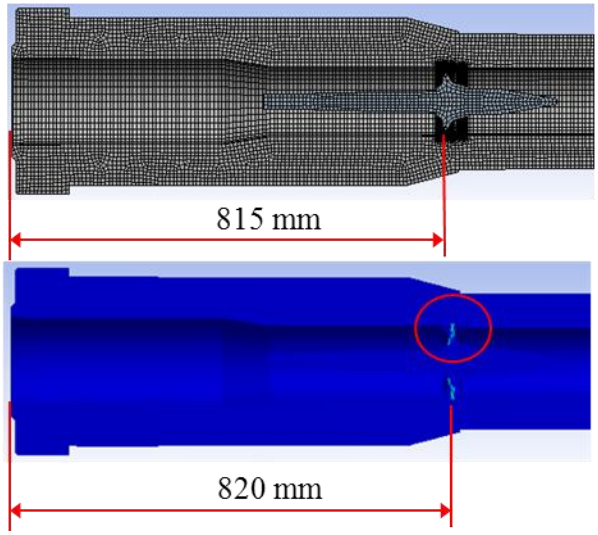

Fig.8: Projectile position before and after ramming

The boundary conditions are set for the problem, including fixed position of the barrel at the barrel bottom and the initial ramming velocity of the projectile. The velocity of the projectile is the velocity of the ramming device at its end position, where the ramming device stops but the projectile moves continuously in the direction of the barrel axis with an initial velocity of 2.9 $m \cdot s^{-1}$.
The first case is described as follows.
The geometry of a new barrel with thermal deformation was established in ANSYS Workbench using FEM. The ramming process of the APFSDS projectile was simulated and calculated on this model base. The position of the projectile before and after ramming, where it is engraved is shown in Fig. 8.

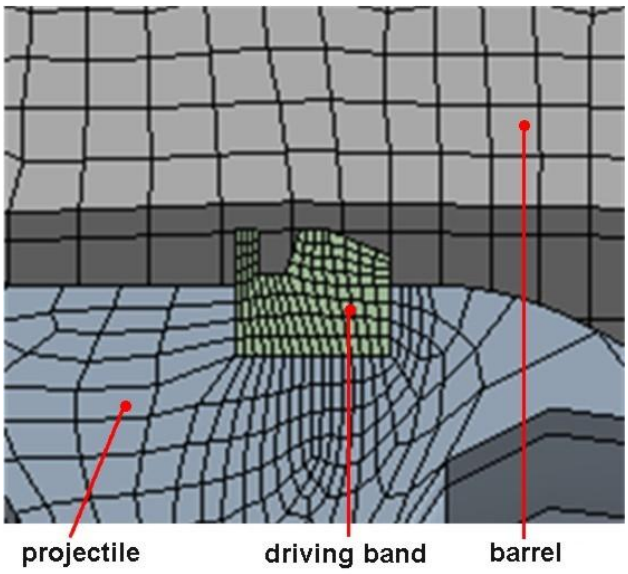

Fig.9: FEM model of driving band engraving

The equivalent stress (Von-Misses) with the thermal deformation effect in the new barrel is 212 MPa. The calculated reaction force achieved at the process beginning is more than 20 kN, see Fig. 10, and the projectile velocity drops after 2 ms approximately, see Fig. 11.

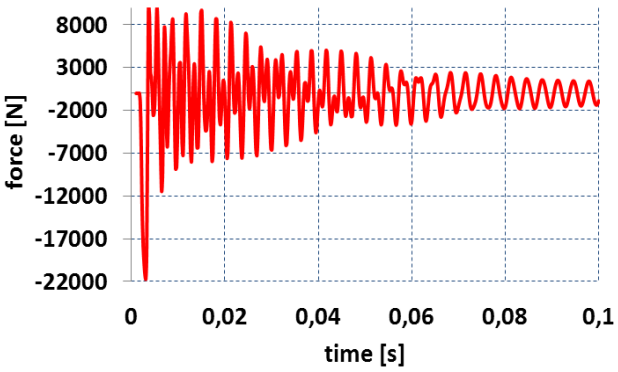

Fig.10: Reaction force in a new barrel

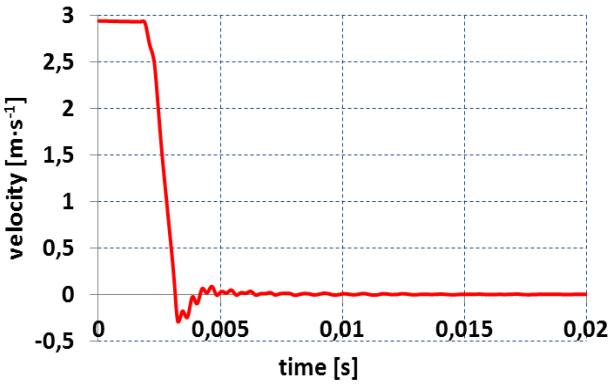

Fig.11: Projectile velocity in a new barrel

ISBN: 978-1-61804-141-8

The second case is described now.
The engraving process was simulated and calculated for the worn barrel including the influences of thermal deformations.

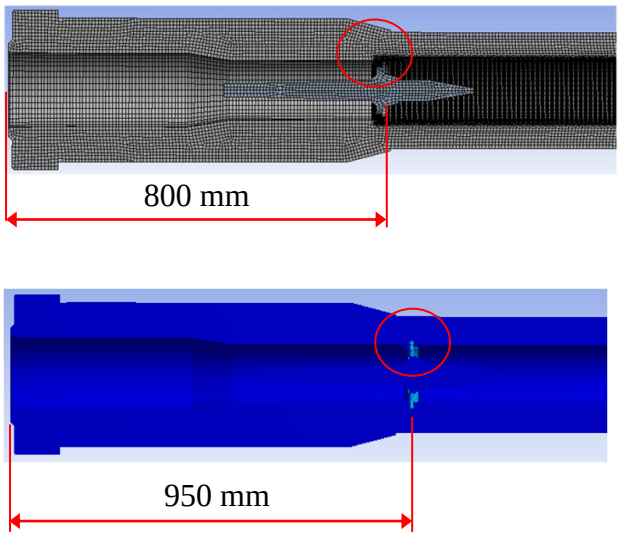

Fig. 12: Projectile position before and after ramming

The maximum equivalent stress in a worn barrel is 98 MPa and that is twice as low as in a new barrel.

The reaction force and the projectile velocity in the engraving process are shown in Fig. 13 and Fig. 14.

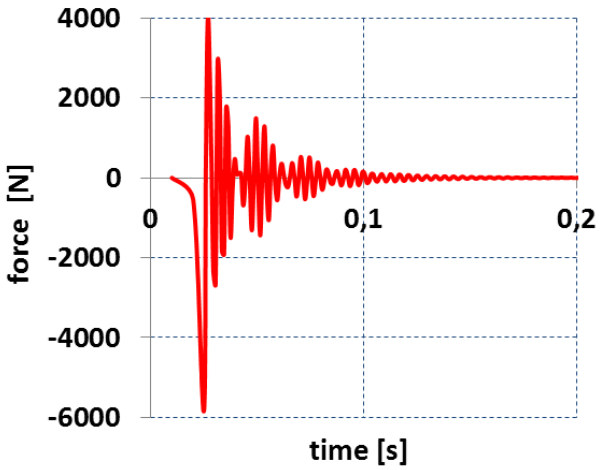

Fig. 13: Reaction force in a worn barrel

The reaction force, securing the projectile in the barrel, is lowered to a similar ratio as the equivalent stress.

According to Fig. 13, and Fig. 14 the engraving process for the worn barrel with thermal deformation effect in the course of a single shot can be evaluated. At the beginning of the engraving period (approximately 0.015 s), the projectile moves without resistance forces as the worn barrel diameter is greater than the driving band diameter. In this stage the projectile velocity slowly decreases from 2.9 $m \cdot s^{-1}$ to 2.5 $m \cdot s^{-1}$, see Fig. 14, as a consequence of action friction forces.

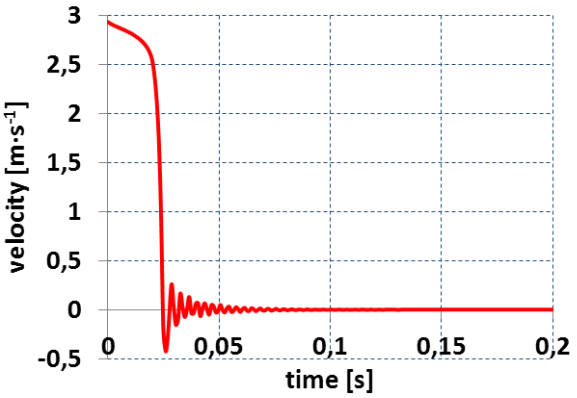

Fig. 14: Projectile velocity in a worn barrel

The resistance force caused by the interaction between the driving band and the inner surface of the barrel - engraving the projectile into the forcing cone - occurs at the point where the barrel diameter is smaller than the driving band diameter. Due to this resistance force the velocity of the projectile decreases dramatically to zero. Simultaneously, due to the driving band dynamic impact to the inner surface of the barrel, both of resistance force and the barrel velocity have vibration forms, see Fig. 10, Fig. 11, Fig. 13, and Fig. 14, as it was confirmed in [8] for similar 155 mm projectiles.

4 Conclusion

For a new barrel, where the barrel dimensions are given in the technical documentation, the distance between the initial projectile position where the impact starts and stops, was 3 – 5 mm. The distance in the worn barrel, as represented in Fig. 8, was much greater than for the new barrel reaching up to 150 mm, see Fig. 12. The prolongation of the ramming displacement leads to a rise in the volume of the barrel chamber causing a change in the development of barrel gas pressure. The place of the maximum value of the gas pressure in the barrel shifts to the place where the barrel thickness is smaller. This phenomenon can cause the risk of barrel chamber elongation. A permanent elongation can occur when the barrel wear is greater than the value specified in the technical documentation of the Czech Defence Standards, see [9] for requirements of the loading process. Then barrel explosion can occur.
The increase in resistance forces, caused by the driving band engraving, happens in the region where

ISBN: 978-1-61804-141-8

the worn barrel diameter is smaller than the driving band diameter. In such a case the projectile is rammed deeper than in an unworn barrel and projectile velocity at the beginning of the engraving is lower as a consequence of the projectile's inertia movement. In a new barrel the rammer is designed to stop its movement at the start of the projectile driving band in the forcing cone. If the rammer stroke was greater rammer deformation could occur. For this reason the rammer velocity was increased up to 3 $m \cdot s^{-1}$. This measure ensured that the projectile would also be held in a worn barrel at any elevation angle when loading on the move where significant inertia forces strongly influence the loading system.

The impact and the interaction between the driving band and the inner barrel surface are non-linear dynamic processes and the velocities and the reaction forces have their typical oscillating movement known as the ping-pong effect, see [16].

In the future, the measuring of reaction forces using the new HBM measuring device and specification of the input data for FEM shall be conducted.

References:

[1] Ogorkiewitz R., *Technology of Tanks I, II*. UK Biddles Limited Guilford and King´s Lynn, 1991.

[2] Peter H., *Armament Engineering a computer aided approach*. Trafford Publishing. Suite 6E. 2333 Government St, Victoria. B.C.V8T 4P4, Canada, ISBN 141200241-9, 282 pages.

[3] Balla J., Jankovych R., Duong V. Y., Interaction between projectile driving band and forcing cone of weapon barrel, *Proceedings of the Applied Computing Conference 2011 (ACC '11),* Angers (France), November 2011, ISBN 978-1-61804-051-0, pp. 194 –199.

[4] Cech V., Kanak J., *Armaments of tank T72*. [Textbook]. Brno Military academy in Brno, 1984, 165 pages.

[5] Balla J., Duong V. Y., Jankovych. R., Evaluation of 152 mm SPH M77 ramming device. In *Proceedings from International Conference on Military Technologies*. Brno University of Defence, 2011, ISBN 978-80-7231-787-5, pp. 1625-1634.

[6] Balla J., Duong V. Y., Jankovych R., Technical Inspection of 125 mm tank cannon ramming device. The *Proceedings from International Conference on Military Technologies*. Brno: University of Defence, 2011, ISBN 978-80-7231-787-5, pp. 1635-1644.

[7] Balla J., Problems of Gun Ammunition Ramming, The Proceedings of IVth European guns and ammunition symposium, Shrivenham: RMCS, UK, SEPT 1997, pp. 35-51.

[8] JN KRIEL & DE MALAN. Measuring some Parameters Relevant to the ballistic Performance of a 155mm Gun System. Somchem, a Division of Denel (Pty) Ltd. South Africa. In: Proceedings of IIIrd European Guns, Mortars and Ammunition Symposium. Shrivenham: RMCS, UK, SEPT 1996.

[9] *Large Calibre Ordnance/Munition Compatibility, Design SafetyRequirements and Safety and Suitability for Service Evaluation* COS 109002 Czech Defence Standard. Prague: MoD, 2005.

[10] Jankovych R., Beer S., T-72 tank barrel bore wear. *International Journal of Mechanics*, Vol. 5, No. 4, 2011, ISSN 1998-4448, pp. 353-360.

[11] Jankovych R., Beer S. Wear of cannon 2A46 barrel bore. The Proceedings of the 2nd International Conference on Theoretical and Applied Mechanics 2011 (TAM '11). Greece, Corfu Island: WSEAS Press, 2011, ISBN 978-1-61804-020-6, pp. 72-76.

[12] *Textbook of Ballistics and Gunnery. Volume One.Part I - Basic theory. Part II - Applications and Design*. London. Her Majesty's Stationnary office, 1987.

[13] Prochazka S., Fiser, M., Skvarek, J. *Barrels*. [Textbook]. University of Defence Brno, 2006, ISBN 80-7231-157-3, 165 pages.

[14] Zienkiewicz O. C., Taylor, R. L., *The finite element method, Volume 1, Basic formulation and linear problem.* Singapore, MacGRAW-HILL International Editions, 1989, 667 pages.

[15] Prochazka, S., Jankovych, R., Semanek, M. Enhancement of system of technical inspections for 2A46 cannon barrel by means of BG-20 device. The Proceedings of ICMT'11 - International Conference on Military Technologies 2011. Brno University of Defence, 2011, ISBN 978-80-7231-787-5, pp. 1785-1792.

[16] Liechti H. A. Ammunition Feeding for Large Calibre Guns. In: The Proceedings of IVth European guns and ammunition symposium, Shrivenham: RMCS, UK, SEPT 1997, pp. 1-34.